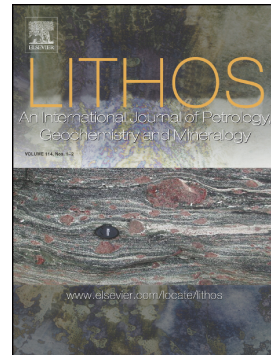


Accepted Manuscript

Neoproterozoic to Cenozoic Magmatism in the central part of the Bohemian Massif (Czech Republic): isotopic tracking of the evolution of the mantle through the Variscan orogeny

Jaroslav Dostal, J. Brendan Murphy, J. Gregory Shellnutt, Jaromír Ulrych, Ferry Fediuk



PII: S0024-4937(18)30490-0

DOI: <https://doi.org/10.1016/j.lithos.2018.12.028>

Reference: LITHOS 4919

To appear in: *LITHOS*

Received date: 31 August 2018

Accepted date: 22 December 2018

Please cite this article as: Jaroslav Dostal, J. Brendan Murphy, J. Gregory Shellnutt, Jaromír Ulrych, Ferry Fediuk , Neoproterozoic to Cenozoic Magmatism in the central part of the Bohemian Massif (Czech Republic): isotopic tracking of the evolution of the mantle through the Variscan orogeny. *Lithos* (2018), <https://doi.org/10.1016/j.lithos.2018.12.028>

This is a PDF file of an unedited manuscript that has been accepted for publication. As a service to our customers we are providing this early version of the manuscript. The manuscript will undergo copyediting, typesetting, and review of the resulting proof before it is published in its final form. Please note that during the production process errors may be discovered which could affect the content, and all legal disclaimers that apply to the journal pertain.

Neoproterozoic to Cenozoic Magmatism in the central part of the Bohemian Massif (Czech Republic): isotopic tracking of the evolution of the mantle through the Variscan orogeny

Jaroslav Dostal^{1*}, J. Brendan Murphy², J. Gregory Shellnutt³, Jaromír Ulrych⁴, Ferry Fediuk⁵

¹Saint Mary's University, Department of Geology, 923 Robie Street, Halifax, Nova Scotia B3H 3C3, Canada

²St. Francis Xavier University, Department of Earth Sciences, Antigonish, Nova Scotia B2G 2W5, Canada

³National Taiwan Normal University, Department of Earth Sciences, 88 Tingzhou Road Section 4, Taipei 11677, Taiwan

⁴Institute of Geology of the Czech Academy of Sciences, Rozvojová 269, CZ-165 02 Prague 6, Czech Republic

⁵Na Petřinách 1897/29, 162 00 Prague 6, Czech Republic

*Corresponding author

E-mail address: jdostal@smu.ca

Abstract

The evolution of the mantle source beneath the Teplá-Barrandian (TBB) and the adjacent southern part of the Saxo-Thuringian (S-STB) and northern part of the Moldanubian (N-MB) blocks of the Bohemian Massif (Czech Republic) is tracked from the Late Neoproterozoic to the Cenozoic in order to examine the coupling between the crust and underlying continental lithospheric mantle (CLM) during the Late Paleozoic Variscan orogeny. In the TBB, Late Neoproterozoic mafic rocks have highly radiogenic Nd but moderately radiogenic Sr isotopes and were derived from a spinel peridotite mantle. These within-plate rocks were emplaced in an intra-oceanic back-arc basin. Early Paleozoic (Ordovician to Early Devonian) mafic rocks are rift/extension-related, enriched in LREE and Nb relative to HREE and were probably derived from a garnet peridotite mantle source. Compared to Neoproterozoic basalts, their $\epsilon_{\text{Nd}}(t)$ values are slightly lower but T_{DM} model ages are indistinguishable suggesting derivation from a deeper portion of the same mantle source. Thus, the weak deformation and low-grade metamorphism associated with the Cadomian orogeny did not significantly decouple the crust from the underlying mantle source beneath the TBB. Early Paleozoic rift-related mafic rocks of the S-STB and N-MB have comparable isotopic signatures indicating a similar mantle source. Late Paleozoic mafic magmatism occurred during the extensional collapse phase of the Variscan orogen, in the aftermath of the collision between Gondwana and Laurussia. The TBB and S-STB basaltic rocks are within-plate, and transitional between alkaline and tholeiitic compositions but show a relative depletion of Nb. Their isotopic characteristics contrast with older basalts in that they have negative $\epsilon_{\text{Nd}}(t)$ values, high initial $^{87}\text{Sr}/^{86}\text{Sr}$ ratios and older T_{DM} model ages (1100 to 1300 Ma). Late Paleozoic mantle-derived potassic-ultrapotassic magmas occurring as lamprophyre dikes and small volume high Mg-K intrusions in N-MB, S-STB and TBB have

similar isotopic characteristics suggesting that all these Late Paleozoic rocks were derived from an old CLM contaminated by fluids or silicic melts derived from subducted Precambrian crustal material or alternatively, the region was underthrust by Gondwanan mantle during the Variscan collision. Cenozoic volcanic rocks in the Bohemian Massif are local representatives of the regionally extensive Cenozoic Central European volcanic province. The rocks are within-plate, alkaline basalts enriched in LREE and Nb and were derived from garnet peridotite mantle. They are significantly more juvenile than Carboniferous-Early Permian mafic rocks, with higher $\epsilon_{\text{Nd}}(t)$ values (typically +3 to +5), lower initial $^{87}\text{Sr}/^{86}\text{Sr}$ ratios and significantly younger T_{DM} age. These data suggest significant input from upwelling asthenospheric mantle, implying that at least a part of the Permian CLM mantle was re-fertilized.

Keywords: Bohemian Massif; Variscan Orogeny; Nd and Sr isotopes; crust; continental lithospheric mantle; rift/extension-related mafic igneous rocks

1. Introduction

Many geochemical and isotopic studies of igneous rocks focus on individual suites that were emplaced within a restricted age range. However, additional insights can be provided by comparing the magmatic characteristics of igneous suites over a range of ages in the same terrane or crustal block (Murphy and Dostal, 2007; Gutiérrez-Alonso et al., 2011; Murphy et al., 2011). For example, by comparing the geochemical and isotopic signatures of mafic magmatism

before and after known collisional events, we can examine the extent of crust-mantle coupling during collisional orogenesis.

In this paper, we use the Teplá-Barrandian (TBB) and adjacent southern part of the Saxon-Thuringian (S-STB) and the northern part of the Moldanubian (N-MB) blocks of the Bohemian Massif (Czech Republic) as an example of this approach. These crustal blocks are widely recognized as the Variscan Suspect Terranes of continental Europe (e.g., Franke, 2000). The Bohemian Massif underwent collisional (Variscan) orogenesis during the Devonian-Early Carboniferous (e.g., Franke, 2000, 2006; Kroner and Romer, 2013). The TBB is one of a few blocks that escaped pervasive reworking during the Paleozoic and preserves a record of magmatism before (Neoproterozoic, Early Paleozoic), during (Late Paleozoic) and after (Cenozoic) the Variscan orogeny.

We combine new geochemical, Sr, and Nd isotopic data with equivalent data from the literature in order to track the evolution of the mantle source beneath the TBB, S-STB and N-MB. This approach complements the recent study by Jastrzębski et al. (2018) by allowing us to: (i) determine the evolution of the mantle source of basalts beneath the TBB and adjacent S-STB and N-MB, (ii) assess how the underlying continental lithospheric mantle (CLM) was affected by collisional orogenesis, and (iii) constrain the timing of any mantle replacement events (MREs, e.g., slab break-off, delamination, re-fertilization) that may have occurred.

2. Geologic Setting

The Late Paleozoic Variscan orogen of continental Europe records the closure of the Rheic Ocean and the collision between Laurussia (Laurentia + Baltica + Avalonia) and Gondwana and was a major event in the amalgamation of Pangea (Franke, 2000; Kroner and Romer, 2013;

Arenas et al., 2014). The Rheic Ocean originated in the late Cambrian-Early Ordovician when terranes, collectively known as peri-Gondwanan terranes (e.g., Ganderia, Carolinia, Avalonia), separated from the northern margin of Gondwana (Murphy et al., 2006; Nance et al., 2010). Their subsequent accretion to Baltica-Laurentia to form Laurussia between the Ordovician and early Devonian resulted in the closure of the Iapetus Ocean and its SE branch -Tornquist Ocean and was a major orogenic event in the development of the Appalachian-Caledonide orogenic belt (e.g., van Staal et al., 2012). The closure of the Rheic Ocean therefore resulted in collision between the northern margin of Gondwana and peri-Gondwanan terranes located along the southern margin of Laurussia (Arenas et al., 2014; Kroner and Romer, 2013).

The Bohemian Massif forms the easternmost part of the European Variscan orogenic belt that stretches across Europe from southeastern Poland through the Czech Republic, northern Austria, Germany and France to northern Spain (Spain/Portugal border; Fig. 1). The belt comprises a collage of terranes that were mainly derived from the northern (African) margin of Gondwana, which underwent gradual rifting since the Late Cambrian due to the opening of the Rheic Ocean (Linnemann et al., 2004, 2010, 2014; Drost et al., 2011; Kroner and Romer, 2013). The individual terranes had complex drift histories, which are still under debate. However, the geological record of the early evolution of the continental lithosphere of these terranes was mostly erased and overprinted during the Variscan orogeny.

The Bohemian Massif (Figs. 1 and 2) is the largest preserved remnant of the Variscan basement in Europe. It consists of four distinct blocks of peri-Gondwanan affinity: Teplá-Barrandian, Brunovistulian (Moravo-Silesian; MSB), Moldanubian (MB) and Saxo-Thuringian (STB) (Franke, 2000). The segments show various degrees of metamorphism and deformation. In most models (e.g., Kroner and Romer, 2013), the Rheic Ocean Suture (Fig. 1) is placed to the

north of the Bohemian Massif, separating the blocks of the Avalonian and Armorician provenances. It wraps around the massif and separates the MB and MSB (Figs. 1 and 2).

In the late Neoproterozoic, as generally accepted, the Bohemian Massif resided along the northern Gondwanan margin, as part of the Avalonian-Cadomian arc (e.g., Linnemann et al., 2004; Drost et al., 2004, 2011). However, the Paleozoic tectonic evolution of the Bohemian Massif (Fig. 2) is highly debated. On one hand, the tectonic boundary between the TBB and MB (e.g., the contact between upper-crustal and mid- to lower crustal rocks; e.g., Faryad and Žák, 2016) is interpreted as a suture reflecting the northwesterly (present coordinates) subduction of an oceanic tract beneath the TBB and the adjacent STB (e.g., Franke, 2000, 2006). This putative oceanic tract has been interpreted to have separated outboard Cadomian terranes from the Gondwanan margin (e.g., Franke, 2000). On the other hand, Schulmann et al. (2009, 2014) invoked the existence of an oceanic tract between the STB (lower plate) and the TBB (upper plate) that was eliminated by southeasterly-directed subduction. In this model, the TBB and the MB preserve different structural levels within the same plate.

Our study focuses on the TBB, which avoided significant Cadomian and Variscan deformation and metamorphism (Pin and Waldhausrová, 2007; Dörr and Zulauf, 2010). Although we cannot distinguish between the two models, we can examine the extent of crust-CLM coupling during the Variscan collisional orogeny by comparing the crustal and mantle sources of Teplá-Barrandian magmatism before and after Variscan collisional events. Since the evolution of the TBB is intertwined with history of adjoining STB and MB and some of our Late Paleozoic and Cenozoic samples were collected just outside of the TBB in the STB, the study also include the S-STB and N-MB.

The TBB forms the central part of the Bohemian Massif and is separated from the surrounding highly metamorphosed segments by major Variscan shear zones (North and West Bohemian shear zones, Zulauf et al., 2002 a,b). To the north, it is in contact with the S-STB (Hajná et al., 2011) and to the south it is surrounded by the MB (Fig. 2). The contact between the TBB and the MB represents the boundary between upper-crustal and mid- to lower crustal rocks (e.g., Faryad and Žák, 2016).

Within the TBB, late Neoproterozoic basement rocks consist of interbedded siliciclastic and volcanic sequences that were weakly deformed and underwent low grade (lower greenschist facies) metamorphism during the Cadomian orogeny. These sequences are unconformably overlain by unmetamorphosed siliciclastic and carbonate sedimentary rocks of Cambrian to Middle Devonian age, which are preserved mainly in the Prague basin (Dörr and Zulauf, 2010). The strata also include interbedded volcanic rocks emplaced in the extensional settings (Patočka et al., 1993; Tasáryová et al., 2018). This Early Paleozoic volcanism, which produced mainly mafic rocks, peaked during the Middle Ordovician (Darriwilian) and Silurian, particularly during Wenlock-Ludlow time. The dating of volcanic activities is based mainly on graptolite biostratigraphy of intercalated sedimentary strata (e.g., Štorch, 1994).

Deformation and metamorphism associated with the Variscan Orogeny began at ca. 380 Ma (Kroner and Romer, 2013; Arenas et al., 2014) and continued until about 300 Ma (Gutiérrez-Alonso et al., 2008, 2011). Orogenic activity was accompanied by the emplacement of various subduction- and extension-related magmas (360-260 Ma – e.g., Lorenz and Nicholls, 1984; Žák et al., 2014). Late orogenic stages were characterized by the formation of large Late Paleozoic volcano-sedimentary basins in the Bohemian Massif including the TBB and S-STB (Ulrych et al., 2002b, 2004, 2006). These basins contain, in the upper parts the continental sediments

(Upper Carboniferous and Lower Permian), which are typically intercalated with volcanic rocks. The Variscan basins are mostly covered by thick Cretaceous sedimentary sequences. However, the stratigraphy, particularly of Westphalian and Stephanian, is well established from numerous drill-holes (e.g., Pešek, 2001). Late orogenic stages in the Bohemian Massif also produced the intrusions of high Mg-K monzonitic/syenitic plutons and lamprophyre and lamproite dikes (Janoušek and Holub, 2007; Krmíček et al., 2016; Kubínová et al., 2017; Soder and Romer, 2018).

After the end of the Variscan orogeny, the Bohemian Massif including parts of TBB and S-STB was transformed into a platform marked by Cretaceous to Quaternary rift-related magmatism (Malkovský, 1987). Most prominent are Cenozoic intraplate alkaline volcanic rocks of the Central European volcanic province, which extends across the Bohemian Massif. Most of the Cenozoic volcanism is spatially and temporally associated with the development of grabens, which are a part of the main rift system (Ulrych et al., 2011). However, there are also numerous examples of the alkaline volcanism occurring at some distance from the main rift system scattered across the northern part of the TBB, S-STB and N-MB (Ulrych et al., 2011).

3. Analytical methods, sampling and alteration

We collected samples of rift-related mafic volcanic rocks from four major episodes of volcanism in the TBB and S-STB: Neoproterozoic, Early Paleozoic, Late Paleozoic and Cenozoic ages, from localities whose geology is well documented. The Neoproterozoic, Early Paleozoic and Cenozoic samples are from outcrops of representative volcanic centres (e.g., Fiala, 1977; Patočka et al., 1993; Ulrych et al., 2011; Dostal et al., 2017). Due to poor surficial exposure, the Late Paleozoic samples are from drill-cores. Geology of the coal-bearing Variscan

basins was investigated in thousands of drill-holes (Ulrych et al., 2006) and several coalmines (Pešek, 2001). The drill-cores provide relatively fresh samples compared to those from outcrops. The locations of sampling sites are given in Appendix 1. As the terrane boundaries are frequently covered by younger (particularly Cretaceous) sediments, locations of some of the Late Paleozoic and Cenozoic samples lie just outside of the TBB, in the southern part of the STB. However, published data (e.g., Ulrych et al. 2002 a,b, 2004, 2006, 2011) show that geochemical characteristics of these samples are closely comparable to the typical rocks of the TBB. The analyses of the Cenozoic rocks were taken from our earlier study (Dostal et al., 2017).

In addition to whole-rock Nd and Sr isotopic data, we also determined major and trace elements abundances to characterize the rocks. Whole rock analyses for major and trace elements (Table 1) were carried out using lithium metaborate - tetraborate fusion at the Activation Laboratories Ltd. in Ancaster, Ontario, Canada. Major elements were determined by an inductively coupled plasma-optical emission spectrometer whereas the determinations of trace elements were done by an inductively coupled plasma-mass spectrometer. Errors obtained during replicate analyses of the international reference standards were between 2% and 8% of the values cited. More information on the major and trace element analyses is available at the Activation Laboratories web site (www.actlabs.com).

The samples were analyzed for Nd and Sr isotopic ratios (Table 2) at the Institute of Earth Sciences, Academia Sinica, Taipei, Taiwan. The detailed procedures are given in Shellnutt et al. (2012). $^{143}\text{Nd}/^{144}\text{Nd}$ ratios were normalized to $^{146}\text{Nd}/^{144}\text{Nd} = 0.7219$ whereas $^{87}\text{Sr}/^{86}\text{Sr}$ ratios were normalized to $^{86}\text{Sr}/^{88}\text{Sr} = 0.1194$. The Nd isotope ratios were determined using a Finnigan Triton thermalionization mass spectrometer, while the Sr isotope ratios were measured by a Finnigan MAT-262. The 2σ values for all samples are given in Table 2. The measured isotope ratios for

the JMC Nd standard is 0.511813 ± 0.000010 (2σ) and for the NBS987 Sr standard is 0.710248 ± 0.00001 (2σ). The initial $^{87}\text{Sr}/^{86}\text{Sr}$ isotopic ratios as well as $\varepsilon_{\text{Nd}}(t)$ values were corrected to the ages given in Table 2. The depleted mantle model ages (T_{DM} ; Table 2) were calculated according to DePaolo (1988). T_{DM} values (Table 2) were not calculated for samples with $^{147}\text{Sm}/^{144}\text{Nd} > 0.165$ as they provide incorrect values (Stern, 2002).

Some investigated Neoproterozoic and Paleozoic rocks were affected to a limited degree by secondary processes including low-grade regional metamorphism and alterations that could have modified their chemical composition. This is indicated by the variable LOI values (weight loss on ignition to 900°C). However, the concentrations of most major elements, high-field-strength elements (HFSE), rare earth elements (REE), Th and transition elements, were probably not affected and are thought to reflect the primary magmatic history of the studied rocks. Similarly, Sm-Nd and Rb-Sr, which are involved in radiogenic isotope systems as parent and daughter isotopes, respectively, as well as Sr and Nd isotopic ratios, display a high degree of chemical congruence, implying relative resistance to secondary processes. Thus, it is inferred that the Nd and probably Sr isotopic values reflect magmatic processes (e.g., Pin and Waldhausrová, 2007).

4. Results

The volcanic activities of the TBB and S-STB can be subdivided into four age stages: Neoproterozoic, Early Paleozoic, Late Paleozoic and Cenozoic.

4.1. Neoproterozoic volcanism

Neoproterozoic mafic volcanism is well preserved in the TBB, and constitutes part of the basement to the Paleozoic Prague basin (Barrandian). The Neoproterozoic basement includes

abundant mafic volcanic rocks (“spilites” of Kettner, 1918). Although the precise age of the sequence is not well-established, available age data indicate that it is late Neoproterozoic (Hajná et al., 2018) and so the sequence provides constraints on the composition of the mantle source during that time interval. Pin and Waldhausrová (2007) reported a Sm-Nd whole rock age of 605 ± 39 Ma for the mafic rocks. Dörr et al (2002) and Drost et al. (2011) obtained a U-Pb detrital zircon age of 585 ± 7 Ma from the uppermost part of the Neoproterozoic sedimentary pile, which provides a minimum age for the mafic rocks. This interpretation is also consistent with the Ar-Ar ages of micas ranging from ~616 to 585 Ma (Sláma et al., 2008). For the purpose of calculating $\varepsilon_{\text{Nd}}(t)$ values, we follow Pin and Waldhauserová (2007) in assuming a depositional age of 600 Ma for our samples (Table 2). Stratigraphic constraints suggest that TB-3 is probably ~ 590 Ma old (V. Kachlík, personal communication).

The mafic volcanic rocks are predominantly basaltic in composition (Table 1), and occur as lava flows and pillow lavas. According to the Nb/Y versus Zr/TiO₂ plot, these volcanic rocks are basalts (Fig. 3) and can be subdivided into two groups (Pin and Waldhausrová, 2007). The first group includes the basalts which have chondrite- and mantle-normalized trace elements patterns depleted in light REE (LREE) relative to heavy REE (HREE) resembling those of N-type MORB (samples TB-1, TB-2; Figs. 4 and 5). Although the mantle normalized trace element plots of our depleted samples do not show negative Nb anomalies, some samples of Pin and Waldhausrová (2007) of this group display a small relative depletion in Nb, probably due to a minor contribution from a subduction process. These features indicate that the Neoproterozoic basalts could have been derived from a depleted lithospheric mantle that was slightly enriched by subduction-related fluids. The rocks of this group have highly radiogenic Nd isotopes ($\varepsilon_{\text{Nd}}(t) \sim +9.1$; Fig. 6, Table 2), comparable to the range reported by Pin and Waldhausrová (2007) (from

+7.8 to +9.3). These values are higher than those of typical depleted mantle reservoir and so their T_{DM} model ages have no geological significance. The initial Sr isotopic ratios spanning from 0.7035 to 0.7047 are elevated compared to the MORB and probably represent a slightly enriched lithospheric mantle source. The second group (samples TB-3, TB-4; Figs. 4 and 5) has trace element patterns characterized by LREE enrichment and the absence of the negative Nb anomaly (Fig. 5). The rocks have geochemical fingerprints of within-plate basalts. Their $\epsilon_{Nd}(t)$ values are also highly radiogenic (~+8.0) and similar to the values reported by Pin and Waldhausrová (2007). The elevated initial $^{87}\text{Sr}/^{86}\text{Sr}$ isotopic ratios (~0.705) mainly reflect a lithospheric mantle source (Fig. 6). The lack of correlations of the Nd isotopic characteristics with Th/Nb and other geochemical signatures corroborates the conclusions of Pin and Waldhausrová (2007) that crustal contamination did not play a significant role during the evolution of the Neoproterozoic rocks. The rather flat HREE part of the chondrite-normalized REE patterns for the basalts implies melting at shallow mantle depths (spinel stability field). Both groups of Neoproterozoic mafic rocks were probably emplaced on a thin continental or oceanic crust and their geochemical signatures reflect the composition of their lithospheric mantle source. Pin and Waldhausrová (2007) inferred that the mafic rocks were emplaced in environments ranging from an intra-oceanic back-arc basin to within-plate settings. This interpretation is compatible with that of Drost et al. (2011) and Linnemann et al. (2010) who interpret Neoproterozoic TBB rocks to have been deposited in a back-arc basin that formed behind the Avalonian-Cadomian arc magmatism that typifies the northern margin of Gondwana.

4.2. Early Paleozoic volcanism

Early Paleozoic volcano-sedimentary sequences of the TBB unconformably overlie the Neoproterozoic basement. The Upper Cambrian igneous activity is represented by subaerial volcanic rocks of the Strašice and Křivoklát-Rokycany volcanic complexes occurring southwest of Prague. The rocks have predominantly intermediate and felsic compositions (Waldhausrova, 1971; Drost et al., 2004; Pin et al., 2007). Rare mafic rocks are rift-related tholeiites (Drost et al., 2004; Pin et al., 2007). Mafic volcanic rocks are particularly well preserved in the rift-related Prague basin where they are interbedded with Early Ordovician to Early Devonian unmetamorphosed fossiliferous sedimentary strata. The basin hosts several volcanic sequences composed of basaltic lavas, minor intrusions, hyaloclastites and volcaniclastic rocks. The cessation of sedimentation in the Prague basin at the beginning of Late Devonian is thought to herald the onset of the Variscan Orogeny (Kachlík and Patočka 1998; Strnad and Mihaljevič 2005). Our mafic rocks, which are from the Prague basin, plot in the alkali basalt field on the Nb/Y versus Zr/TiO₂ graph (Fig. 3). The basalts have high contents of MgO (6-10 wt. %). Sample TB-8 (Tables 1 and 2), which has very high MgO (>20 wt. %) is meimechite, which is an olivine-rich cumulate rock (Tasáryová et al., 2018). The chondrite-normalized REE patterns are distinctly enriched in LREE and linear with $(\text{La}/\text{Yb})_{\text{n}} \sim 4-10$ and without any noticeable Eu anomalies (Fig. 4). The basalts were probably derived from a garnet-bearing mantle source. The primitive mantle-normalized plots of these within-plate basalts do not show negative Nb anomalies (Fig. 5). The meimechite displays a similar pattern but has lower absolute contents of incompatible trace elements compared to the others.

Our $\epsilon_{\text{Nd}}(t)$ values of Early Paleozoic rocks (+6.8 to +4.9) overlap data of Vokurka and Frýda (1997) and Tasáryová et al. (2018) for equivalent rocks of the Prague basin. Although they are close to depleted mantle compositions, the $\epsilon_{\text{Nd}}(t)$ values are lower than those of Neoproterozoic

mafic rocks (+9.3 to +7.8; Table 2), but they do have similar T_{DM} model ages. The initial $^{87}\text{Sr}/^{86}\text{Sr}$ ratios (0.7047 to 0.706) are, on average, slightly higher than the values of Neoproterozoic basalts (Table 2; Fig. 6). There are no indications that the Early Paleozoic rocks were affected by crustal contamination, an interpretation consistent with the observations of Patočka et al. (1993) and Tasárová et al. (2018). The trace element and isotopic characteristics of the mafic volcanic rocks suggest that they were derived from a deeper (garnet peridotite) portion of the same mantle as the Neoproterozoic basalts. This interpretation implies that the weak deformation and lower greenschist facies metamorphism during the Cadomian orogeny did not significantly decouple the crust from the mantle source beneath the TBB.

The Nd isotopic characteristics of these TBB basaltic rocks are comparable to the Early Paleozoic extension-related rocks of the S-STB. These S-STB metamorphosed basaltic rocks have a chemical composition ranging from N-MORB (Ślęża and N. Ruda ophiolites, Kryza and Pin, 2010) with $\varepsilon_{\text{Nd}}(t) \sim +7.8$ to +8.7 to tholeiitic and alkali basalts (Crowley et al. 2002; Dostál et al., 2001; Furnes et al., 1994; Hegner and Kröner, 2000; Kryza and Pin, 2002; Pin et al., 2007) with $\varepsilon_{\text{Nd}}(t)$ typically $\sim +5.6$ to +8.8 and T_{DM} (mostly ~ 600 -800 Ma). The Early Paleozoic metamorphosed mafic rocks of the N-MB have also similar Nd isotopic signatures with $\varepsilon_{\text{Nd}}(t) \sim +4.5$ to +9 (Janoušek et al., 2008).

4.3. Late Paleozoic volcanism

Late Paleozoic magmatic activities of the Bohemian Massif are related to the last stages of the Variscan orogeny, particularly Variscan orogenic collapse. The principal Variscan collision (360-290 Ma) was followed at ca. 290 Ma by extension associated with crustal thinning that was accompanied by volcanic activity (Scholle et al., 1995). A recent study by Jastrzębski et al.

(2018) emphasizes the importance of structures in the ascent of magmas from their crustal and mantle sources. The orogenic collapse of thickened crust during the late stages of the Variscan orogeny in the Bohemian Massif led to the development of continental intra-montane limnic basins. The main periods of volcanic activity in these basins took place during the Upper Carboniferous and Lower Permian (peaking in the Autunian). In the basins, the volcanic complexes are interstratified with the sedimentary successions. The volcanic complexes are composed of lavas, sub-volcanic intrusions (sills) and volcaniclastic deposits including large volumes of ignimbrites occurring close to the boundary between TBB and S-STB. Some of these subvolcanic intrusions are up to 100 m thick and tens of km long (Ulrych et al., 2006). With the exception of Ar-Ar and K-Ar methods, there are relatively few radiometric ages available (e.g., Opluštil et al., 2016a,b). The ages of volcanic activities within the basins are usually constrained by geologic and stratigraphic evidence.

The volcanic sequences are typically bimodal. On the Nb/Y versus Zr/TiO₂ plot, the mafic rocks straddle the boundary between alkaline and subalkaline basalts (Fig. 3). Mafic rocks are within-plate basalts, basaltic andesites or basaltic trachyandesites whereas the felsic members are rhyolites or trachytes (Ulrych et al., 2004). The chondrite normalized REE patterns of the mafic rocks are fractionated with $(La/Yb)_n \sim 7-10$ and show small negative Eu anomalies (Fig. 4). Their primitive mantle-normalized graphs display negative Nb anomalies (Fig. 5) that suggest either contamination of mantle by continental crust en route to the surface or pre-melting contamination of the mantle source by subduction components. Unlike the other TBB and S-STB volcanic suites, the latest Carboniferous-Early Permian mafic rocks have negative $\epsilon_{Nd}(t)$ values (Table 2; Figs. 6 and 7). The values are comparable to the data reported by Ulrych et al. (2002b, 2004, 2006) from the Late Paleozoic basins elsewhere in the Bohemian Massif. Their Nd model

ages yield values of about 1100 to 1300 Ma (Fig. 8) suggesting the involvement of Precambrian material in the source of these rocks. Such a process is also consistent with high initial $^{87}\text{Sr}/^{86}\text{Sr}$ ratios ranging from 0.707 to 0.7085 (Table 2; Fig. 6). The high Sr isotopic ratios suggest the contamination of the mantle source by sedimentary material (Fig. 6). The lack of correlations of SiO_2 and MgO with $\epsilon_{\text{Nd}}(t)$ values as well as other geochemical parameters indicates that the negative Nb anomaly reflects the source composition rather than crustal contamination. This interpretation is also supported by geochemical and isotopic similarities of the mafic rocks from various Late Paleozoic basins of the Bohemian Massif (Ulrych et al., 2004, 2006) whereas the contamination is a random process and should produce notable scatter of the data.

The Bohemian Massif hosts numerous mantle-derived potassio-ultrapotassio igneous rocks which include lamprophyre and lamproite dikes and minor intrusions of high Mg-K diorite/monzonite dated mostly at 300-330 Ma (Abdeldadil et al., 2014; Adwankiewicz, 2007; Gerdes et al., 2000; Janoušek et al., 1995; Krmíček et al., 2016; Soder and Romer, 2018). These rocks have $\epsilon_{\text{Nd}}(t)$ values ranging typically from -3 to -6 and $T_{\text{DM}} \sim 800\text{-}1200$ Ma. These Nd isotopic signatures overlap those of the basalts but differ from the Early Paleozoic mafic rocks of the central part of the Bohemian Massif including TBB, S-STB and N-MB.

4.4. Cenozoic volcanism

Cenozoic intraplate alkaline volcanic rocks of the Bohemian Massif belong to the easternmost part of the Late Cretaceous to Cenozoic Central European volcanic province (CEVP), which extends from France across Germany to the Czech Republic and Poland. In the Bohemian Massif, most of the volcanism is associated with the Ohře/Eger graben along the re-activated suture zone between TBB and STB, although numerous volcanic complexes are scattered across

parts of the TBB, S-STB and N-MB (e.g., Ulrych et al., 2011). The volcanic complexes are composed of lava flows, volcano-sedimentary and volcaniclastic deposits and subvolcanic intrusions. The volcanic rocks are a rift-related, alkaline silica-undersaturated series. The dominant mafic rock types are basanites and trachybasalts (typically with > 7 wt. % MgO); felsic types (phonolites and trachytes) are subordinate. The volcanic activities lasted from 79 Ma to < 1 Ma (Ulrych et al., 2008, 2011).

The major and trace element compositions of the volcanic rocks are similar to those of alkaline intraplate rocks worldwide (e.g., Greenough et al., 2005a,b; Lustrino and Wilson, 2007). The mafic rocks have subparallel chondrite-normalized REE patterns, which are linear, enriched in LREE with high $(La/Yb)_n$ and lack noticeable negative Eu anomalies (Fig. 4). The primitive mantle-normalized trace element patterns of the mafic rocks (Fig. 5) display a shape common among primitive alkali basaltic rocks from both continental and oceanic environments (Lustrino and Wilson, 2007) including ocean island basalts. These patterns peak at Nb indicating the mafic rocks were not significantly contaminated by crustal material and implying that their geochemical characteristics probably reflect those of their mantle source. Cenozoic basalts are more juvenile than Carboniferous–Early Permian mafic rocks, with higher $\varepsilon_{Nd}(t)$ values (+1.8 to +4.3), lower initial $^{87}\text{Sr}/^{86}\text{Sr}$ isotopic ratios (0.7034 to 0.7046; Fig. 6; Table 2) and significantly lower T_{DM} ages, mostly between 300-400 Ma (Fig. 8). These isotopic values are comparable to many other data reported from the Cenozoic volcanic rocks from the Bohemian Massif (Adwandkiewicz et al., 2016; Alibert et al., 1987; Bendl et al., 1993; Blusztajn and Hart, 1989; Hasse and Renno, 2008; Holub et al., 2010; Lustrino and Wilson, 2007; Ulrych et al., 2002a, 2008, 2011), which typically have $\varepsilon_{Nd}(t) \sim +3$ to +5. The mantle source of the Cenozoic volcanic

rocks was garnet peridotite that showed subtle heterogeneity in modal and Nd isotopic compositions (Dostal et al., 2017).

5. Summary and Discussion

A synoptic analysis of suites of different ages in the same orogen provides insights into the coupling between the crust and mantle over time when combined with regional geological constraints. In locations where collisional orogenesis has occurred, this approach can distinguish regions where the crust and lithospheric mantle remained coupled from regions where they became detached. In addition, the chemical characteristics inherited by basalt from a putative CLM source can be distinguished from those whose petrogenesis has been influenced by mantle replacement events such as slab break-off, delamination, or re-fertilization or by fluids and silicic melts derived from subducted sediments.

The Teplá-Barrandian crustal block is particularly suited to this approach because it is one of a few blocks that escaped pervasive reworking during the Paleozoic and preserves a record of magmatism before (Neoproterozoic, Early Paleozoic), during (Late Paleozoic) and after (Cenozoic) the Variscan orogeny. Although all four magmatic stages generated within-plate basalts, there are significant differences among these rocks.

Neoproterozoic mafic rocks have geochemical and Nd-Sr isotopic compositions typical of arc-back arc complexes and are consistent with models that place the Bohemian Massif within the Avalonian-Cadomian magmatic arcs along the northern margin of Gondwana (e.g., Linnemann et al., 2004; Drost et al., 2004). Early Paleozoic (Ordovician-Devonian) alkali mafic rocks were probably derived from a garnet peridotite mantle source. Although $\epsilon_{\text{Nd}}(t)$ values are slightly lower, T_{DM} model ages are indistinguishable suggesting derivation from a deeper

(garnetperidotite) portion of the same mantle as the Neoproterozoic basalts. Thus, the weak deformation and low grade metamorphism associated with the Cadomian orogeny did not significantly decouple the crust from the mantle source beneath the TBB.

The geochemical and isotopic characteristics of the Late Paleozoic mafic rocks imply that their CLM source was significantly different from the sources of the Neoproterozoic and Early Paleozoic and Cenozoic basaltic rocks. Compared to those rocks, the Carboniferous-Early Permian mafic rocks have significantly lower (-2.6 to -3.7) $\epsilon_{\text{Nd}}(t)$ values (Figs. 6 and 7) but significantly higher T_{DM} ages (Fig. 8) and initial Sr isotopic ratios. The lower $\epsilon_{\text{Nd}}(t)$ values of the Late Paleozoic basaltic volcanic rocks are typical of lithospheric mantle and are indistinguishable from the CLM documented beneath Avalonia (e.g., Fig. 7; Murphy and Dostal, 2007), a peri-Gondwanan terrane that was located on the southern Laurussian margin during the development of the Variscan orogen, and are interpreted to reflect the composition of Avalonian CLM.

There are two possible explanations for the contrasting isotopic values. First, the mafic rocks may have been derived from older CLM. The $\epsilon_{\text{Nd}}(t)$ values are similar to those found in mafic magmas derived from the northern margin of Gondwana (e.g., Gutiérrez-Alonso et al., 2011). This explanation requires that the mantle beneath the Bohemian Massif was replaced by old CLM during the Carboniferous, implying that the region was underthrust by Gondwanan mantle during Variscan collision. The mantle-normalized patterns of the mafic rocks with negative Nb and Ti anomalies and LILE enrichment relative to HREE (Fig. 5) would imply that subduction-related processes modified the old Gondwanan mantle. Alternatively, the negative $\epsilon_{\text{Nd}}(t)$ values together with the higher depleted mantle model ages could be attributed to a mantle contaminated by Precambrian crustal material. The mafic magmatism is approximately coeval

with localized mantle-derived potassic-ultrapotassic mafic (high Mg-K monzonites, lamprophyres and lamproites) magmatism which occurs along the margins of the TBB or within the unit and within the S-STB and N-MB, and have similar isotopic characteristics (e.g., Janoušek and Holub, 2007; Krmíček et al., 2016; Soder and Romer, 2018; Jastrzebski et al., 2018) to the studied Late Paleozoic volcanic rocks. The differences among these rock-types may be attributed to the varying amount of subducted continental material (mainly sediments) which would have controlled the trace element and isotopic signature of the source. In this scenario, the lithospheric mantle source of the Late Paleozoic rocks would have been variably contaminated by fluids and silicic magmas derived from the dehydration and melting of subducted continental material (e.g., Soder and Romer, 2018). To distinguish between these two scenarios, an orogen-scale examination of the covariation of Nd-Sr isotopic systematics with trace elements is required.

As our data cannot constrain subduction zone polarity, we present a schematic cartoon that shows the general environment that generated the Late Paleozoic volcanic and intrusive rocks (Fig. 9) involving contamination of the lithospheric mantle by dehydration and melting of subducted Precambrian sediments.

Irrespective of which Late Paleozoic scenario is correct, the higher $\varepsilon_{\text{Nd}}(t)$ values and lower initial Sr isotopic ratios in the Cenozoic volcanic rocks suggest input from upwelling asthenospheric mantle implying that at least the lower (garnet peridotite) Permian CLM mantle was re-fertilized by upwelling asthenosphere. The Cenozoic rocks of the Bohemian Massif are local representatives of the Central European volcanic province, suggesting that the re-fertilization was a regional event across continental Europe (e.g., Hoernle et al., 1995).

The mantle sources beneath the TBB, N-MB and S-STB show similar evolution, implying that the central part of the Bohemian Massif has comparable mantle characteristics with changes from a juvenile mantle source for the Early Paleozoic mafic rocks through an enriched lithospheric mantle source for the Late Paleozoic rocks to the juvenile source of Cenozoic basaltic rocks.

Acknowledgements

We thank Drs. Nelson Eby, John Greenough and Václav Kachlík for their constructive reviews. JD and JBM acknowledge the continuing support of NSERC, Canada, and Randy Corney for technical assistance. This research was also supported by the institutional project RVO 67985831 of the Institute of Geology of the Czech Academy of Sciences to JU and by MOST (Taiwan) grant 106-2116-M-003-007 to JGS.

References

- Abdelfadil, K.M., Romer, L.R., Glodny, J., 2014. Mantle wedge metasomatism revealed by Li isotopes in orogenic lamprophyres. *Lithos* 196-197, 14-26.
- Alibert, C., Leterrier, J., Panasiuk, M., Zimmermann, J.L., 1987. Trace and isotope geochemistry of the alkaline Tertiary volcanism in southwestern Poland. *Lithos* 20, 311-321.
- Arenas, R., Díez Fernández, R., Sánchez Martínez, S., Gerdes, A., Fernández-Suárez, J., Albert, R., 2014. Two-stage collision: exploring the birth of Pangea in the Variscan terranes. *Gondwana Research* 25, 756-763.

Awdankiewicz, M., 2007. Late Palaeozoic lamprophyres and associated mafic subvolcanic rocks of the Sudetes (SW Poland): petrology, geochemistry and petrogenesis. *Geologia Sudetica* 39, 11-97.

Awdankiewicz, M., Rapprich, V., Miková, J., 2016. Magmatic evolution of compositionally heterogeneous monogenetic Cenozoic Strzelin volcanic field (Fore-Sudetic Block, SW Poland). *Journal of Geosciences* 61, 425-450.

Bendl, J., Vokurka, K., Sundvoll, B., 1993. Strontium and Neodymium isotope study of Bohemian basalts. *Mineralogy and Petrology* 48, 35-45.

Blusztajn, J., Hart, S.R., 1989. Sr, Nd and Pb isotopic character of Tertiary basalts from southwest Poland. *Geochimica et Cosmochimica Acta* 53, 2689-2696.

Crowley, Q.G., Timmermann, H., Noble, S.R., Holland, J.G., 2002. Palaeozoic terrane amalgamation in Central Europe: a REE and Sm-Nd isotope study of the pre-Variscan basement, NE Bohemian Massif. *Geological Society, London, Special Publication* 201, 157-176.

DePaolo, D.J., 1988. Neodymium isotope geochemistry: an introduction. Springer Verlag, New York, 187 p.

Dörr, W., Zulauf, G., 2010. Elevator tectonics and orogenic collapse of a Tibetan-style plateau in the European Variscides: the role of the Bohemian shear zone. *International Journal of Earth Sciences* 99, 299-325.

Dörr, W., Zulauf, G., Fiala, J., Franke, W., Vejnar, Z., 2002. Neoproterozoic to Early Cambrian history of an active plate margin in the Teplá-Barrandian unit - A correlation of U-Pb isotopic dilution-TIMS ages. *Tectonophysics* 352, 65-85.

- Dostal, J., Patočka, F., Pin, C., 2001. Middle/Late Cambrian intracontinental rifting in the central West Sudetes, NE Bohemian Massif (Czech Republic): geochemistry and petrogenesis of the bimodal metavolcanic rocks. *Geological Journal* 36, 1-17.
- Dostal, J. Shellnutt, J.G., Ulrych J., 2017. Petrogenesis of the Cenozoic alkaline volcanic rock series of the České Středohoří complex (Bohemian Massif), Czech Republic: a case for two lineages. *American Journal of Science* 317, 677-706.
- Drost, K., Linnemann, U., McNaughton, N., Fatka, O., Kraft, P., Gehmlich, M., Tonk, C., Marek, J., 2004. New data on the Neoproterozoic-Cambrian geotectonic setting of the Teplá-Barrandian volcano-sedimentary successions: U-Pb zircon ages, and provenance (Bohemian Massif, Czech Republic). *International Journal of Earth Sciences* 93, 742-757.
- Drost, K., Gerdes A., Jeffries T., Linnemann U., Storey C., 2011. Provenance of Neoproterozoic and early Paleozoic siliciclastic rocks of the Teplá-Barrandian Unit (Bohemian Massif): evidence from U-Pb detrital zircon ages. *Gondwana Research* 19, 213-231.
- Faryad, S.W., Žák, J., 2016. High-pressure granulites of the Podolsko complex, Bohemian Massif: An example of crustal rocks that were subducted to mantle depths and survived a pervasive mid-crustal high-temperature overprint. *Lithos* 246-247, 246-260.
- Fiala, F., 1977. The Upper Proterozoic volcanism of the Barrandian area and problem of spilites. *Sborník Geologických Věd, Geologie* 30, 2-247.
- Franke, W., 2000. The mid-European segment of the Variscides: tectonostratigraphic units, terrane boundaries and plate tectonic evolution. *Geological Society, London, Special Publications* 179, 35-61.

Franke, W., 2006. The Variscan orogen in Central Europe: construction and collapse. In: Gee, D.G., Stephenson, R.A. (Eds.), European Lithosphere Dynamics. Geological Society, London, Memoirs 32, 333-343.

Furnes, H., Kryza, R., Muszyński, A., Pin, C., Garmann, L.B., 1994. Geochemical evidence for progressive rift-related volcanism in the eastern Variscides. Journal of the Geological Society of London 151, 91-109.

Gerdes, A., Wörner, G., Finger, F., 2000. Hybrids, magma mixing and enriched mantle melts in post-collisional Variscan granitoids: the Rastenberg pluton, Austria. Geological Society, London, Special Publications 179, 415-431.

Greenough, J.D., Dostal, J., Mallory-Greenough, L.M., 2005a. Oceanic Island Volcanism I: Mineralogy and Petrology. Geoscience Canada 32, 29-45.

Greenough, J.D., Dostal, J., Mallory-Greenough, L.M., 2005b. Oceanic Island Volcanism II: Mantle Processes. Geoscience Canada 32, 77-90.

Gutiérrez-Alonso, G., Fernández-Suárez, J., Weil, A.B., Murphy, J.B., Nance, R.D., Corfú, F., Johnston, S.T., 2008. Self-subduction of the Pangean global plate. Nature Geoscience 1, 549-553, doi:10.1038/ngeo250.

Gutiérrez-Alonso, G., Murphy, J.B., Fernández-Suárez, J., Weil, A.B., Franco, M.P., Gonzalo, J.C., 2011. Lithospheric delamination in the core of Pangea: Sm-Nd insights from the Iberian mantle. Geology 39, 155-158.

Hajná J., Žák J., Kachlík, V., 2011. Structure and stratigraphy of the Teplá–Barrandian Neoproterozoic, Bohemian Massif: a new plate-tectonic reinterpretation. Gondwana Research 19, 495-508.

- Hajná J., Žák J., Dörr, W., Kachlík, V., Sláma, J., 2018. New constraints from detrital zircon ages on prolonged, multiphase transition from the Cadomian accretionary orogeny to a passive margin of Gondwana. *Precambrian Research* 317, 159-178.
- Haase, K.M., Renno, A.D., 2008. Variation of magma generation and mantle sources during continental rifting observed in Cenozoic lavas from the Eger Rift, Central Europe. *Chemical Geology* 257, 195-205.
- Hegner, E., Kröner, A., 2000. Review of Nd isotopic data and xenocrystic and detrital zircon ages from the pre-Variscan basement in the eastern Bohemian Massif: speculation on palinspastic reconstructions. *Geological Society, London, Special Publications*, 179, 113-129.
- Hoernle, K., Zhang, Y-S., Graham, D., 1995. Seismic and geochemical evidence for large-scale mantle upwelling beneath the eastern Atlantic and western and central Europe. *Nature* 374, 34-39.
- Holub, F.V., Rapprich, V., Erban, V., Pécsay, Z., Mlčoch, B., Míková, J., 2010. Petrology and geochemistry of the Tertiary alkaline intrusive rocks at Dourov, Dourovské hory volcanic complex (NW Bohemian Massif). *Journal of Geosciences* 55, 251-278.
- Janoušek, V., Rogers, G., Bowls, D. R., 1995. Sr-Nd isotopic constraints on the petrogenesis of the Central Bohemian Pluton, Czech Republic. *International Journal of Earth Sciences* 84, 520-534.
- Janoušek, V., Vrána, S., Erban, V., Vokurka, K., Drábek, M., 2008. Metabasic rocks in the Varied Group of the Moldanubian Zone, southern Bohemia-their petrology, geochemical character and possible petrogenesis. *Journal of Geosciences* 53, 31-46.

- Janoušek, V., Holub, F., 2007. The causal link between HP-HT metamorphism and ultrapotassic magmatism in collisional orogens: case study from the Moldanubian Zone of the Bohemian Massif. *Proceedings of the Geologists' Association* 118, 75-86.
- Jastrzębski, M., Machowiak, K., Krzeminska, E., Farmer, G.L., Larionov, A.N., Murtezi, M., Majka, J., Sergeev, S., Ripley, E.M., Whitehouse, M., 2018. Geochronology, petrogenesis and geodynamic significance of the Visean igneous rocks in the Central Sudetes, northeastern Bohemian Massif. *Lithos* 316-317, 385-405.
- Kachlík, V., Patočka, F., 1998. Cambrian/Ordovician intracontinental rifting and Devonian closure of the rifting generated basins in the Bohemian Massif realms. *Acta Universitatis Carolinae, Geologica* 42, 433-441.
- Kettner, R., 1918. Versuch einer Stratigraphischen Einteilung des Böhmischen Algonkium, *Geologische Rundschau* 8, 169-188.
- Krmíček, L., Romer, R.L., Ulrych, J., Glodny, J., Prelević, D., 2016. Petrogenesis of orogenic lamproites of the Bohemian Massif. Sr-Nd-Pb-Li isotopic constraints for Variscan enrichment of the ultra-depleted mantle domains. *Gondwana Research* 35, 198-216.
- Krøner, U., Romer, R.L., 2013. Two plates - Many subduction zones: The Variscan orogeny reconsidered. *Gondwana Research* 24, 298-329.
- Kryza, R., Pin, C., 2002. Mafic rocks in a deep crustal segment of the Variscides (the Góry Sowie, SW Poland): evidence for crustal contamination in an extensional setting. *International Journal of Earth Sciences* 91, 1017-1029.
- Kryza, R., Pin, C., 2010. The Central-Sudetic ophiolites (SW Poland): petrogenetic issues, geochronology and palaeotectonic implications. *Gondwana Research* 17, 292–305.

- Kubínová, Š., Faryad, S. W., Verner, K., Schmitz, M., Holub, F., 2017. Ultrapotassic dykes in the Moldanubian Zone and their significance for understanding of the post-collisional mantle dynamics during Variscan orogeny in the Bohemian Massif. *Lithos* 272-273, 205-221.
- Linnemann, U., McNaughton, N.J., Romer, R.L., Gehmlich, M., Drost, K., Tonk, C., 2004. West African provenance for Saxo-Thuringia (Bohemian Massif): did Armorica ever leave pre-Pangean Gondwana? U/Pb-SHRIMP zircon evidence and the Nd-isotopic record. *International Journal of Earth Sciences* 93, 683-705.
- Linnemann, U., Hofmann, M., Romer, R.L., Gerdes, A., 2010. Transitional stages between the Cadomian and Variscan orogenies: basin development and tectonomagmatic evolution of the southern margin of the Rheic Ocean in the Saxo-Thuringian Zone (North Gondwana shelf). In: Linnemann, U., Romer, R.L. (Eds.), *Pre-Mesozoic Geology of Saxo-Thuringia - From the Cadomian Active Margin to the Variscan Orogen*. Schweizerbart, Stuttgart, pp. 59-98.
- Linnemann, U., Gerdes, A., Hofmann, M., Marko, L., 2014. The Cadomian Orogen: Neoproterozoic to Early Cambrian crustal growth and orogenic zoning along the periphery of the West African Craton-Constraints from U-Pb zircon ages and Hf isotopes (Schwarzburg Antiform, Germany). *Precambrian Research* 244, 236-278.
- Lorenz, V., Nicholls, I.A., 1984. Plate and intraplate processes of Hercynian Europe during the late Paleozoic. *Tectonophysics* 107, 25-56.
- Lustrino, M., Wilson, M., 2007. The circum-Mediterranean anorogenic Cenozoic igneous province. *Earth Science Reviews* 81, 1-65.
- Malkovský, M., 1987. The Mesozoic and Tertiary basins of the Bohemian Massif and their evolution. *Tectonophysics* 137, 31- 42.

Murphy, J.B., Dostal, J., 2007. Continental mafic magmatism of different ages in the same terrane: Constraints on the evolution of an enriched mantle source. *Geology* 35, 335-338.

Murphy, J.B., Dostal, J., Gutierrez-Alonso, G., Keppie, J.D., 2011. Early Jurassic magmatism on the northern margin of CAMP: derivation from a Proterozoic sub-continental lithospheric mantle. *Lithos* 123, 158-164.

Murphy, J.B., Gutierrez-Alonso, G., Nance, R.D., Fernandez-Suarez, J., Keppie, J.D., Quesada, C., Strachan, R.A., Dostal, J., 2006. Origin of the Rheic Ocean: rift along a Neoproterozoic suture? *Geology* 34, 325-328.

Nance, R.D., Gutierrez-Alonso, G., Keppie, J.D., Linnemann, U., Murphy, J.B., Quesada, C., Strachan, R.A., Woodcock, N., 2010. Evolution of the Rheic Ocean. *Gondwana Research* 17, 194 -222.

Opluštil, S., Schmitz, M., Kachlik, V., Štamberg, S., 2016a. Re-assessment of lithostratigraphy, biostratigraphy, and volcanic activity of the Late Paleozoic Intra-Sudetic, Krkonoše-Piedmont and Mnichovo Hradiště basins (Czech Republic) based on new U-Pb CA-ID-TIMS ages. *Bulletin of Geosciences* 91, 399-432 (Czech Geological Survey, Prague).

Opluštil, S., Schmitz, M., Cleal, C.J., Martínek, K., 2016b. A review of the Middle-Late Pennsylvanian west European regional substages and floral biozones, and their correlation to the Geological Time Scale based on new U-Pb ages. *Earth-Science Reviews* 154, 301-335.

Patočka, F., Vlašimský, P., Blechová, K., 1993. Geochemistry of Early Paleozoic volcanics of the Barrandian Basin (Bohemian Massif, Czech Republic): implications for paleotectonic reconstruction. *Jahrbuch der Geologischen Bundesanstalt, Wien*, 136, 873-896.

- Patočka, F., Dostal, J., Pin, C., 1997. Early Palaeozoic intracontinental rifting in the central west Sudetes, Bohemian Massif: geochemical and Sr–Nd isotopic study on felsic-mafic metavolcanics of the Rýchory Mts Complex. *Terra Nova Abstracts Supplement* 1, 144–145.
- Pešek, J., 2001. Geology and deposits of the Upper Palaeozoic limnic basins of the Czech Republic. Czech Geological Survey. Prague, 243 p. (in Czech)
- Pin, C., Waldhausrová, J., 2007. Sm-Nd isotope and trace element study of Late Proterozoic metabasalts (“spilites”) from the Central Barrandian Domain (Bohemian Massif, Czech Republic). In: Linnemann, U., Nance, R.D., Kraft, P., Zulauf, G., (Eds.), *The evolution of the Rheic Ocean: from Avalonian-Cadomian Active Margin to Alleghenian-Variscan Collision*. Geological Society of America, Special Paper 423, 231-247.
- Pin, C., Kryza, R., Oberc-Dziedzic, T., Mazur, S., Turniak, K., Waldhausrová, J., 2007. The diversity and geodynamic significance of Late Cambrian (ca. 500 Ma) felsic anorogenic magmatism in the northern part of the Bohemian Massif: A review based on Sm-Nd isotope and geochemical data. In: Linnemann, U., Nance, R.D., Kraft, P., Zulauf, G. (Eds.), *The evolution of the Rheic Ocean: from Avalonian-Cadomian Active Margin to Alleghenian-Variscan Collision*. Geological Society of America, Special Paper 423, 209-229.
- Scholle, P., Peryt, T.M., Ulmer-Scholle, D.S., 1995. *The Permian of Northern Pangea*, vol. 1, Springer, Berlin, 261 p.
- Schulmann, K., Konopásek, J., Janoušek, V., Lexa, O., Lardeaux, J.M., Edel, J.B., Štípská, P., Ulrich, S., 2009. An Andean type Palaeozoic convergence in the Bohemian Massif. *Comptes Rendus Geoscience* 341, 266-286.

- Schulmann, K., Lexa, O., Janoušek, V., Lardeaux, J.M., Edel, J.B., 2014. Anatomy of a diffuse cryptic suture zone: an example from the Bohemian Massif, European Variscides. *Geology* 42, 275-278.
- Shellnutt, J.G., Bhat, G.M., Wang, K.L., Brookfield, M.E., Dostal, J., Jahn, B.-M., 2012. Origin of the silicic volcanic rocks of the Early Permian Panjal traps, Kashmir, India. *Chemical Geology* 334, 154-170.
- Sláma, J., Dunkley, D.J., Kachlík, V., Kusiak, M.A., 2008. Transition from island-arc to passive setting on the continental margin of Gondwana: U-Pb zircon dating of Neoproterozoic metaconglomerates from the SE margin of the Teplá-Barrandian Unit, Bohemian Massif. *Tectonophysics* 461, 44-59.
- Soder, C.G., Romer, R.L., 2018. Post-collisional Potassic - Ultrapotasssic Magmatism of the Variscan Orogen: Implications for Mantle Metasomatism during Continental Subduction. *Journal of Petrology* 59, 1007-1034.
- Stern, R.J., 2002. Crustal evolution in the East African Orogen: a neodymium isotopic perspective. *Journal of African Earth Sciences* 34, 109-117.
- Štorch, P., 1994. Graptolite biostratigraphy of the Lower Silurian (Llandovery and Wenlock) of Bohemia. *Geological Journal* 29, 137-165.
- Strnad, L., Mihaljevič, M., 2005. Sedimentary provenance of Mid-Devonian clastic sediments in the Teplá-Barrandian Unit (Bohemian Massif): U-Pb and Pb-Pb geochronology of detrital zircons by laser ablation ICP-MS. *Mineralogy and Petrology* 84, 47-68.
- Sun, S. S., McDonough, W. F., 1989. Chemical and isotopic systematics of oceanic basalts: implications for mantle composition and processes. *Geological Society London, Special Publication* 42, 313-345.

- Tasáryová, Z., Janoušek, V., Frýda, J., 2018. Failed Silurian continental rifting at the NW margin of Gondwana: evidence from basaltic volcanism of the Prague Basin (Teplá-Barrandian Unit, Bohemian Massif). International Journal of Earth Sciences 107, 1231-1266.
- Ulrych, J., Svobodová, J., Balogh, K., 2002a. The source of Cenozoic volcanism in the České středohoří Mts., Bohemian Massif. Neues Jahrbuch für Mineralogie, Abhandlungen 177, 133-162.
- Ulrych, J., Štěpánková, J., Novák, J.K., Pivec, E., Prouza, V., 2002b. Volcanic activity in Late Variscan Krkonoše Piedmont Basin: petrological and geochemical constraints. Slovak Geological Magazine 33, 219-235.
- Ulrych, J., Fediuk, F., Lang, M., Martinec, P., 2004. Late Paleozoic volcanic rocks of the Intra-Sudetic Basin, Bohemian Massif: Petrological and geochemical characteristics. Chemie der Erde 64, 127-153.
- Ulrych, J., Pešek, J., Štěpánková-Svobodová, J., Bosák, P., Lloyd, F.E., von Seckendorff, V., Lang, M., Novák, J.K., 2006. Permo-Carboniferous volcanism in late Variscan continental basins of the Bohemian Massif (Czech Republic): geochemical characteristic. Chemie der Erde 66, 37-56.
- Ulrych, J., Dostal, J., Hegner, E., Balogh, K., Ackerman, L., 2008. Late Cretaceous to Paleocene melilitic rocks of the Ohře/Eger Rift in northern Bohemia, Czech Republic: Insights into the initial stages of continental rifting. Lithos 101, 141-161.
- Ulrych, J., Dostal, J., Adamovič, J., Jelínek, E., Špaček, P., Hegner, E., Balogh, K., 2011. Recurrent Cenozoic volcanic activity in the Bohemian Massif (Czech Republic). Lithos 123, 133-144.

- van Staal, C.R., Barr, S.M., Murphy, J.B., 2012. Provenance and tectonic evolution of Ganderia: constraints on the evolution of the Iapetus and Rheic oceans. *Geology* 40, 987-990.
- Vokurka, K., Frýda, J., 1997. The neodymium isotopes in Lower Paleozoic basalts from the Barrandian (Teplá–Barrandian Unit, Bohemian Massif). *Geoscience Research Report* 1996, p. 87 (in Czech).
- Waldhausrová, J. 1971. The chemistry of the Cambrian volcanics in the Barrandian area. *Krystalinikum* 8, 45-75.
- White, W. M., Dupré, B., 1986. Sediment subduction and magma genesis in the Lesser Antilles: isotopic and trace element constraints. *Journal of Geophysical Research* 91, 5927-5941.
- Winchester, J. A., Floyd, P.A., 1977. Geochemical discrimination of different magma series and their differentiation products using immobile elements. *Chemical Geology* 20, 325-343.
- Zulauf, G., Bues, C., Dörr, W., Vejnar, Z., 2002a. 10 km Minimum throw along the West Bohemian shear zone: Evidence for dramatic crustal thickening and high topography in the Bohemian Massif (European Variscides). *International Journal of the Earth Sciences* 91, 850-864.
- Zulauf, G., Dörr, W., Fiala, J., Kotková, J., Maluski, H., Valverde-Vaquero, P., 2002b. Evidence for high-temperature diffusional creep preserved by rapid cooling of lower crust (North Bohemian shear zone, Czech Republic). *Terra Nova* 14, 343-354.
- Žák, J., Verner, K., Janoušek, V., Holub, F.V., Kachlík, V., Finger, F., Hajná, J., Tomek, F., Vondrovic, L., Trubač, J. 2014. A plate-kinematic model for the assembly of the Bohemian Massif constrained by structural relationships around granitoid plutons. *Geological Society, London, Special Publications* 405, 169-196.

Figure captions

Fig. 1. Sketch map of the Variscan belt in Europe with the Rheic Suture. Modified after Krmíček et al. (2016). TBB-Teplá-Barrandian block; MB- Moldanubian block; STB- Saxo-Thuringian block and MSB-Brunovistullian (Moravo-Silesian) block.

Fig. 2. Geological map of the Bohemian Massif with a regional subdivision. Major Cadomian and Variscan granitoid intrusions are shown for reference. Modified after Krmíček et al. (2016).

Fig. 3. Nb/Y versus Zr/TiO₂ classification graph of Winchester and Floyd (1977) for the mafic rocks of the TBB and S-STB showing Neoproterozoic, Early Paleozoic, Late Paleozoic and Cenozoic rocks. Alk-Bas, alkali basalt; Bsn, basanite; Nph, nephelinite; TrachyAnd, trachyandesite; Com, comendite; Pant, pantellerite.

Fig. 4. Chondrite-normalized REE abundances of the mafic rock rocks of the TBB and S-STB. Normalizing values are after Sun and McDonough (1989).

Fig. 5. Primitive-mantle normalized trace element abundances of mafic rocks of the TBB and S-STB. Normalizing values are after Sun and McDonough (1989).

Fig. 6. $\varepsilon_{\text{Nd}}(t)$ versus initial $^{87}\text{Sr}/^{86}\text{Sr}$ ratios (Table 2) for volcanic rocks of the Bohemian Massif showing the field for mid-ocean ridge basalts (MORB). The enriched mantle EMI and EMII members as well as the HIMU member and the horizontal and vertical Bulk Silicate Earth (BSE) lines are shown for comparison. Sediments - after White and Dupré (1986).

Fig. 7. $\varepsilon_{\text{Nd}}(t)$ versus time graph comparing new Nd isotopic data for the mafic rocks of the TBB and S-STB with a field of the Nd isotopic data for the Avalonian basement and CLM (after Murphy et al., 2011). Note the two Neoproterozoic symbols reflect four samples due to overlap.

Fig. 8. Graph showing the depleted mantle model ages (T_{DM} in Ma) of the mafic rocks of the TBB and S-STB. The model ages calculated according to DePaolo (1988).

Fig. 9. Schematic section showing a possible tectonic scenario affecting the central part of the Bohemian Massif during the Late Paleozoic Variscan orogeny. The isotopic signature of the mantle could be explained either by underthrusting of Gondwanan mantle and/or by contamination of the mantle wedge by fluids and melts derived from subducted sediments.

Table 1. Major and trace element composition of mafic rocks of the Teplá-Barrandian Block

		Neoproterozoic				Early Paleozoic					
Sample# (wt.%)		TB-1	TB-2	TB-3	TB-4		TB-6	TB-7	TB-8	TB-9	TB-10
SiO ₂		51. 49	.6 0	47 7	58 2	44	44. 50	45. 37	39. 20	.3 8	44. 84
TiO ₂		0.8 0	1. 03	0. 57	1. 89		3.2 6	2.0 0	1.5 5	3. 09	1.7 9
Al ₂ O ₃		16. 40	.9 2	15. 7	14. 5		15. 60	14. 73	7.3 4	.3 3	15. 53
Fe ₂ O ₃ *		7.8 8	.4 1	10. 9	10. 04		12. 45	12. 78	16. 98	.2 4	11. 19
MnO		0.1 3	0. 17	0. 13	0. 13		0.1 7	0.1 7	0.2 0	0. 14	0.1 5
MgO		5.7 0	6. 95	3. 63	3. 71		6.5 0	9.4 6	22. 45	6. 82	7.7 5
CaO		12. 48	.9 9	2. 51	.2 7	11. 12	9.8 9	5.3 8	3.7 3	9. 07	8.2 1
Na ₂ O		3.3 0	2. 58	4. 69	3. 99		2.7 9	3.6 5	0.8 7	2. 28	3.2 6
K ₂ O		0.4 3	0. 08	1. 22	0. 15		0.8 1	0.4 8	0.2 7	0. 79	0.6 4
P ₂ O ₅		0.0 5	0. 11	0. 09	0. 28		0.2 0	0.1 4	0.1 2	0. 52	0.1 8
LOI		1.5 5	2. 98	3. 46	8. 12		4.4 8	6.3 6	7.8 5	3. 74	5.8 2
Σ		100 .22	.8 2	.7 3	.3 5	99 98	100 .65	100 .52	100 .56	.4 1	99. 36
Mg#		0.5 9	0. 57	0. 40	0. 48		0.5 1	0.5 9	0.7 2	0. 51	0.5 8
Cr (ppm)		430	39 0	10	19 0		200	390	150 0	27 0	28 0
Ni		120	11 0	10	11 0		60	130	610	19 0	13 0
Co		49	44	24	33		43	59	117	52	51
Sc		40	42	32	30		27	19	18	22	25
V		264	27 8	26 1	22 9		322	258	206	26 4	23 9
Rb		5	1	15	3		8	8	6	6	10
Cs		0.5	0. 1	0. 9	0. 8		0.1	0.2	2.3	0. 8	1.9
Ba		464	14	52 6	15 7		861	138 5	176 8	61 7	99 3
Sr		140	22 8	11 7	39 7		522	658	118	11 47	91 0
Ga		18	19	15	16		27	18	12	24	21
Ta		0.1 8	0. 28	0. 37	1. 02		1.3 2	0.7 7	0.6 8	2. 66	1.1 0

Nb		5.4	6.0	6.3	16.1		17.2	11.2	9.6	34.7	16.2
Hf		1.1	2.0	1.7	3.7		3.4	2.3	1.7	5.4	2.8
Zr		28	70	53	2	15		120	71	55	20
Y		22	32	19	33		20	16	11	25	18
Th		0.3	0.6	2.37	1.33	25		1.10	0.87	0.77	2.41
U		0.3	0.4	1.16	0.55	45		0.36	0.34	0.27	0.093
La		1.5	3.2	8.42	12.23	.7	12.0	7.60	6.04	27.4	11.1
Ce		4.7	9.2	18.93	30.0	.7	27.9	17.4	13.6	59.4	24.3
Pr		0.8	1.6	2.70	4.31	46		3.88	2.42	1.86	7.79
Nd		4.8	9.6	9.44	20.32	.3	18.0	10.6	8.57	33.0	13.9
Sm		1.8	3.8	2.29	5.46	09		4.85	2.95	2.26	7.22
Eu		0.7	1.4	0.39	1.73	95		1.74	1.16	0.81	2.35
Gd		2.8	4.7	2.52	5.76	67		4.64	3.32	2.43	6.83
Tb		0.5	0.8	0.84	0.50	97		0.74	0.55	0.41	0.099
Dy		3.8	5.5	3.42	5.21	87		4.16	3.18	2.26	5.22
Ho		0.8	1.0	0.11	0.66	18		0.74	0.59	0.42	0.94
Er		2.2	3.9	2.16	3.01	35		1.91	1.56	1.07	2.40
Tm		0.3	0.5	0.48	0.33	50		0.26	0.22	0.15	0.33
Yb		2.2	3.5	2.13	3.23	22		1.62	1.38	0.96	1.98
Lu		0.3	0.3	0.46	0.34	47		0.24	0.21	0.14	0.29

Fe_2O_3^* - total Fe as Fe_2O_3 ; LOI - loss on ignition; Mg# = $\text{MgO}/(\text{MgO}+\text{FeO}^*)$ mol%

Table 1. Major and trace element composition of mafic rocks of the TBB and S-STB (Contd.)

Sample# (wt.%)	Late Paleozoic					Cenozoic					TB-28
	TB-11	TB-12	TB-13	TB-14	TB-15	TB-21	TB-22	TB-23	TB-24	TB-27	
SiO_2	59.64	43.57	50.09	48.84	42.07	40.91	41.34	41.13	30.56	53.76	45.18
TiO_2	1.24	1.11	1.52	2.09	1.37	3.88	3.73	3.03	2.28	1.15	3.59
Al_2O_3	15.40	12.30	14.98	15.29	16.36	14.35	10.32	13.93	7.38	17.89	15.49
Fe_2O_3^*	7.46	11.61	10.10	10.35	9.04	12.81	10.24	12.83	11.58	5.58	10.82
MnO	0.11	0.17	0.16	0.10	0.36	0.20	0.13	0.23	0.20	0.20	0.18

MgO	2.50	11.0	6	4.97	4.92	5.26		7.39	12.6	1	7.40	17.0	1	1.43	5.40
CaO	5.39	6.61		8.81	5.71		10.0	12.4	13.1	9	13.36	21.1	0	5.58	10.60
Na ₂ O	3.45	1.78		2.83	3.06	4.07		3.67	0.78		1.53	0.52	4.53		3.38
K ₂ O	2.58	0.69		1.29	2.65	0.22		2.00	0.97		1.82	0.75	3.95		1.96
P ₂ O ₅	0.44	0.31		0.53	0.64	0.40		0.74	0.26		1.11	1.12	0.32		0.51
LOI	2.46	9.52		3.56	4.99	9.32		0.00	5.55		4.29	6.27	4.11		3.27
Σ	100.6	98.7		98.8	98.6	98.4		98.3	99.1		100.6	98.7	98.4		100.3
	7	3		4	4	8		9	1		6	7	9		8
Mg#	0.40	0.65		0.49	0.48	0.54		0.53	0.71		0.53	0.74	0.34		0.50
Cr (ppm)	40	290		140	190	190		40	690		140	810	10		40
Ni	30	260		70	90	60		60	180		70	330	10		70
Co	19	65		33	32	35		46	56		40	59	7		30
Sc	15	21		25	24	26		28	49		25	23	3		24
V	114	161		200	188	206		426	369		322	252	111		378
Rb	63	20		34	72	3		43	164		121	26	113		84
Cs	7.9	1.5		0.8	21.7	0.2		0.4	0.6		2.0	0.5	1.5		1.4
Ba	704	288		571	798	213		576	1002		575	717	1388		776
Sr	299	270		328	362	279		967	613		981	1799	1492		904
Ga	23	15		21	24	21		25	18		23	18	32		24
Ta	2.00	1.11		1.82	2.18	1.48		7.17	3.34		6.77	10.7	7.34		5.50
Nb	30.5	17.1		27.4	34.1	23.1		89.7	45.3		101	151	147		78.0
Hf	7.5	4.1		6.9	9.1	4.9		6.7	4.5		6.2	5.5	12.8		8.1
Zr	274	143		268	359	183		259	137		239	247	605		329
Y	43	27		43	51	36		30	13		32	29	29		22
Th	12.5	3.21		5.75	7.75	5.54		7.17	2.82		7.89	23.0	17.2		8.90
U	3.01	0.59		0.98	1.63	1.65		2.06	0.81		2.23	4.83	3.92		3.10
La	55.9	26.5		45.8	59.3	35.3		68.9	25.7		71.7	163	106		50.8
Ce	114	55.2		95.1	126	74.0		134	53.0		140	304	177		105
Pr	13.9	6.78		11.6	15.6	9.25		16.2	6.70		16.2	33.8	17.8		12.4
Nd	52.4	26.7		45.4	63.0	37.0		62.0	26.8		61.3	120	56.9		47.4
Sm	9.55	5.59		9.12	12.6	7.50		11.3	4.96		10.5	18.4	8.49		8.50
Eu	1.95	1.60		2.24	2.85	1.85		3.27	1.53		3.24	5.13	2.53		2.53
Gd	8.81	5.32		8.16	10.5	6.88		8.68	4.02		8.70	12.9	6.46		6.50
Tb	1.42	0.89		1.36	1.67	1.13		1.18	0.60		1.21	1.53	0.91		0.90
Dy	7.78	4.97		7.68	9.32	6.54		6.01	2.94		6.42	7.08	5.09		4.60
Ho	1.53	0.96		1.46	1.80	1.33		1.04	0.48		1.19	1.11	0.97		0.80
Er	4.22	2.84		4.18	5.08	3.60		2.71	1.21		3.06	2.61	2.66		2.20
Tm	0.64	0.42		0.65	0.76	0.52		0.36	0.16		0.40	0.30	0.38		0.30
Yb	3.94	2.80		4.09	4.70	3.40		2.17	0.95		2.55	1.63	2.61		1.80
Lu	0.57	0.41		0.60	0.69	0.48		0.29	0.12		0.34	0.21	0.38		0.26

Fe₂O₃* - total Fe as Fe₂O₃; LOI - loss on ignition; Mg# = MgO/(MgO+FeO*) mol%

Table 2. Sr and Nd isotopic composition of mafic rocks of the TBB and S-STB

S a m p i e	A g (N a)	R b (p p m)	S r (p p m)	⁸ 7	⁸⁷	⁸⁷	N d (p p m)	S m (p p m)	¹⁴⁷	S m ¹⁴ ⁴ N d	143	Nd/ ¹⁴⁴	143	ϵ Nd (t)	T D M (N a)	
Neoproterozoic																
T B - 1	6 0 0	1 4 5	0 0 0	0 .1 3	0. 70 00	0. 70 06	4 7 6	4 1 6	1 0. 8	0. 23 39	0.5 0.5 56	0.5 132 6	0.5 33 2	12 33 9	9	
T B - 2	6 0 0	2 2 1	0 1 8	0 3 3	0. 70 23	0. 70 23	3 5 4	9 3 4	3 0. 9	0. 21 07	0.5 131 59	0.5 33 1	0.5 11 1	12 33 9	9	
T B - 3	6 0 0	1 1 5	0 1 7	0 3 1	0. 70 84	0. 70 15	5 2 1	9 2 2	2 0. 3	0. 15 96	0.5 129 01	0.5 129 01	0.5 27 3	12 27 0	8 4 2	
T B - 4	6 0 0	3 9 3						2 0 3	5 .0 9	0. 15 16	0.5 128 65	0.5 26 9	0.5 26 9	12 26 9	4 7 1	
Early Paleozoic																
T B - 6	4 2 5	5 2 8	0 4 2	0 66 3	0. 70 63	0. 70 22	6 3 2	1 8 0	4 .8 5	0. 16 29	0.5 127 94	0.5 127 94	0.5 34 1	12 34 9	4 6 6	
T B - 7	4 4 5	6 5 8						1 0 6	2 .9 5	0. 16 83	0.5 128 17	0.5 32 17	0.5 32 16	12 32 6	5 7 8	

T B -	4 4 8	4 1 5	6 1 8	0 .1 7	0. 70 59 57	0. 70 0 50 25	8 .2 5 7	2 .0. 2 6	0. 15 94	0.5 128 21	0.5 12 35 6	5 5 7	6 4 8	
T B -	4 2 9	1 4 0	0 1 7	0 0 5	0. 70 47 52	0. 70 46 61	3 3 0	7 .2 26	0. 13 26	0.5 128 07	0.5 12 44 3	6 6 8	4 6 8	
T B -	4 1 0	3 1 0	9 1 0				1 3 9	3 .5 2	0. 15 31	0.5 128 21	0.5 12 38 7	6 8 0	5 8 5	
Late Paleozoic														
T B -	2 1 1	9 6 3	2 9 9	0 1 0	0. 6 01 01	0. 70 75 66 77	5 2 5 4	9 .5 11 50	0. 0. 11 02	0.5 123 09	0.5 12 09 8	- 3 2	1 0 3	
T B -	2 1 2	9 2 7	2 7 0	0 1 4	0. 01 99	0. 70 88 93	7 6 5 7	2 .5 12 9	5 0. 12 66	0.5 123 69	0.5 12 12 3	- 2 1	1 8 9	
T B -	2 1 3	9 3 5	3 2 4	0 0 8	0. 0. 80 94	0. 70 88 26	7 8 5 6	0 5 1 4	0 0. 12 14	0.5 123 54	0.5 12 12 0	- 2 1	1 3 8	
T B -	3 1 4	0 7 0	3 6 2	0 7 6	0. 70 95 91	0. 70 11 34	7 1 3 0	0 2 1 6	0. 0. 12 09	0.5 123 20	0.5 12 08 3	- 3 1	1 8 7	
T B	2 9	2 3	0 7	0. .70	0. 0.	0. 70	3 7	7 .12	0. 12	0.5 123	0.5 12	- 3	1 2	

-15	8	9	031	8701	08569	.	0	5	25	02		063	.	377
Cenozoic														
TB-21	6.225	4.379	0.19	0.7023515	0.703504	0.705200	0.701103	0.7003	0.512787	0.512782	0.512780	0.512781	0.512780	0.512781
TB-22	3.16.00	1.6143	0.7739	0.703983	0.703609	0.7026.98	0.70196	0.7019	0.512793	0.512788	0.512784	0.512789	0.512784	0.512789
TB-23	2.8.71	1.921	0.357	0.704458	0.704311	0.704610	0.7040.10	0.704536	0.512841	0.512822	0.512823	0.512826	0.512823	0.512826
TB-24	6.8.4.6	8.020	0.144	0.703396	0.703355	0.701802	0.700928	0.700928	0.512782	0.512770	0.512770	0.512772	0.512770	0.512772
TB-27	3.1.1.0	1.421	0.219	0.704736	0.704639	0.70586.99	0.7044.49	0.704903	0.51271	0.512692	0.512692	0.512880	0.512692	0.512880
TB-22	2.4.7	8.046	0.26	0.7044602	0.7047004	0.7057744	0.70480.5	0.704585	0.512751	0.512733	0.512735	0.512755	0.512735	0.512755

8				9			3												
							0												
							8												

m-measured;
i-initial

Highlights

- Isotopic tracking of the evolution of the mantle of the Bohemian Massif
- Coupling between the crust and underlying lithospheric mantle
- Nd and Sr isotope variations related to the Variscan Orogeny
- Neoproterozoic to Cenozoic rift-related basaltic rocks

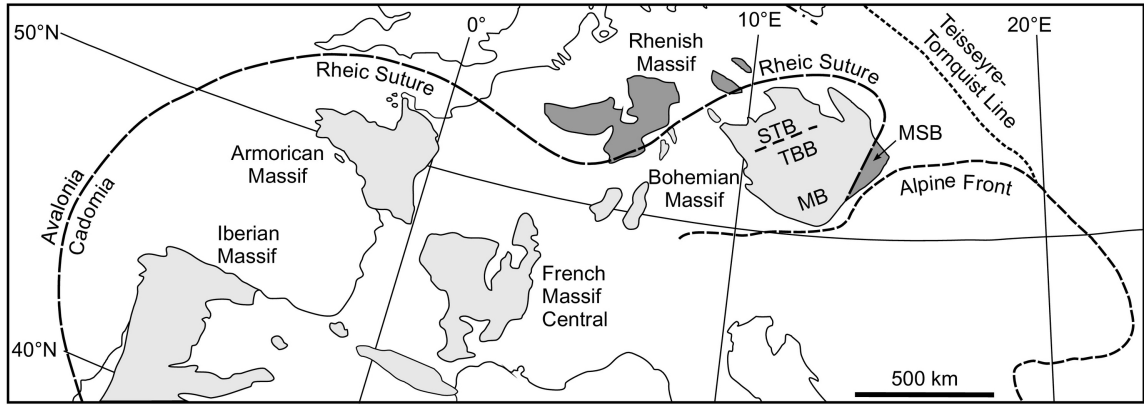


Figure 1

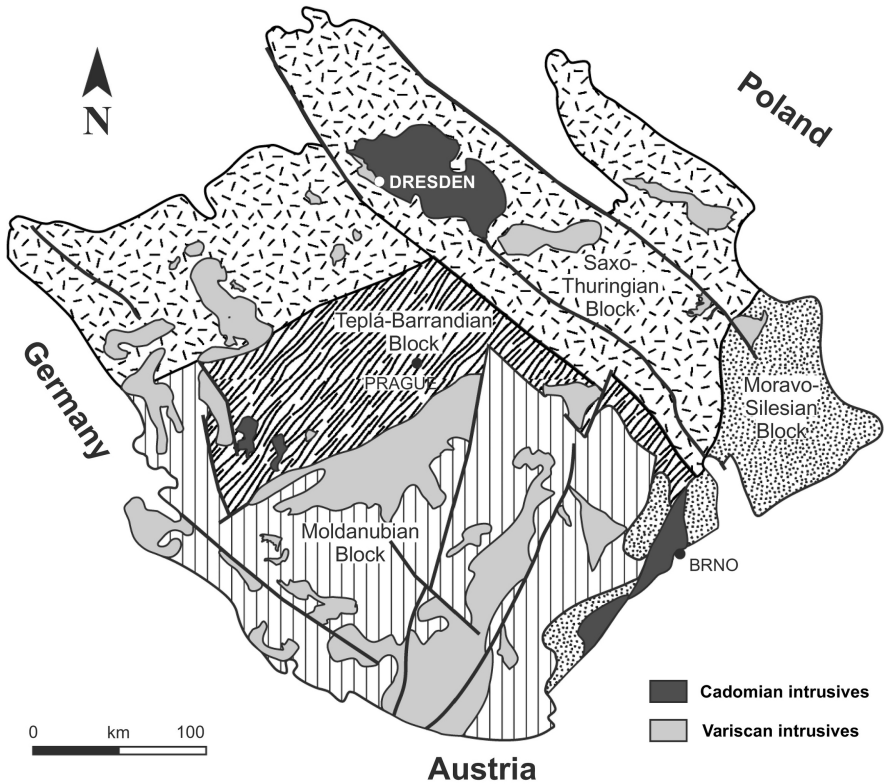


Figure 2

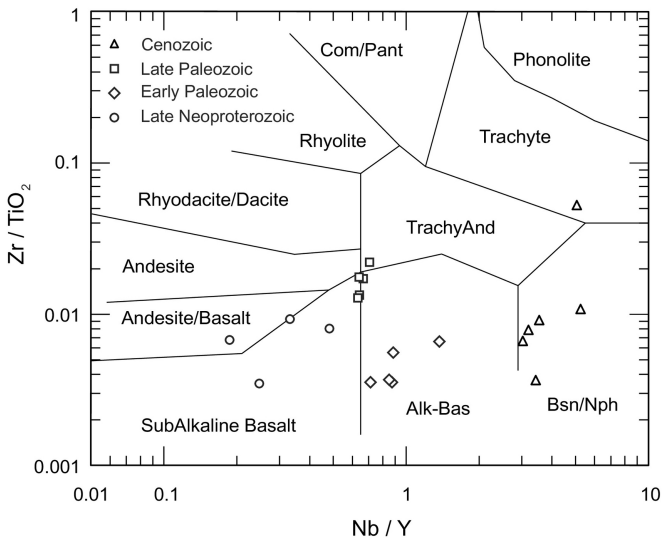


Figure 3

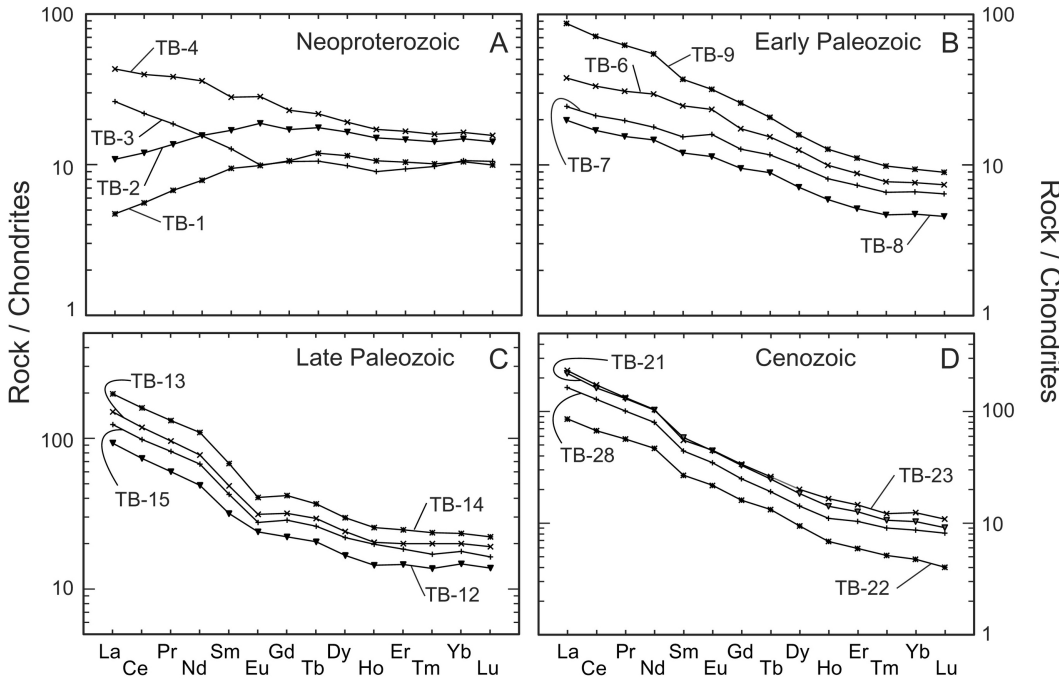


Figure 4

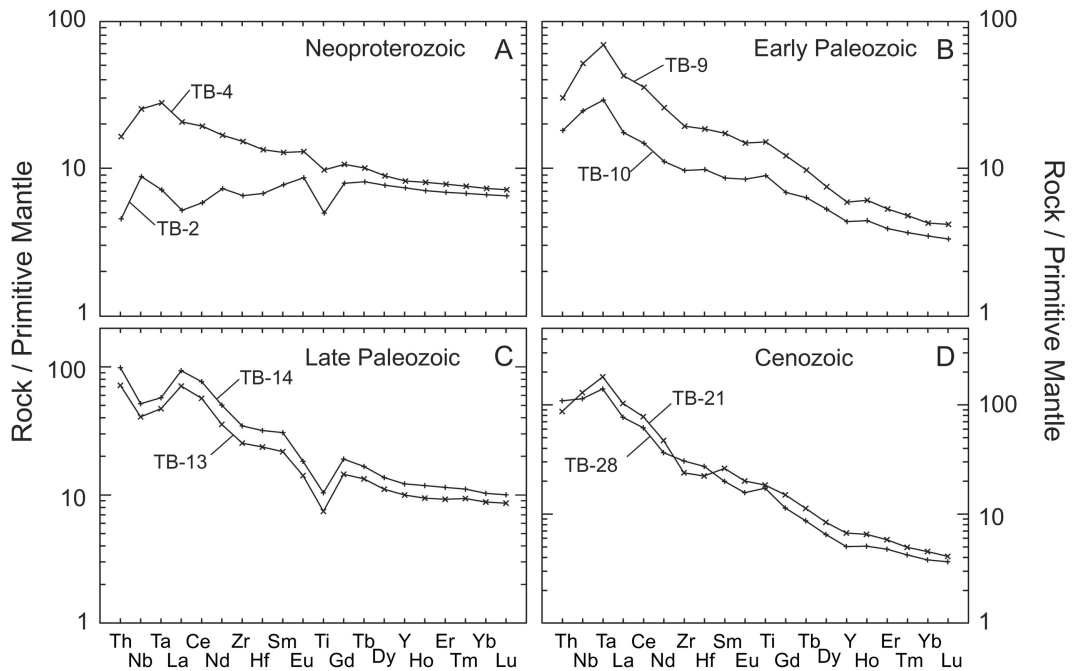


Figure 5

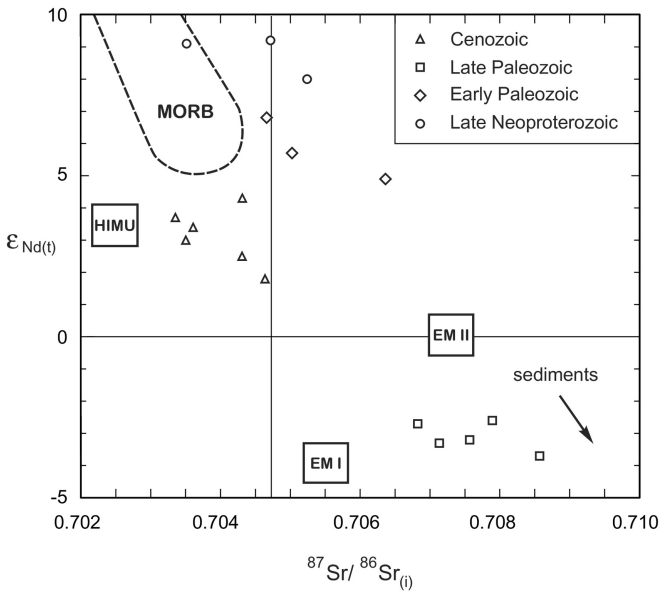


Figure 6

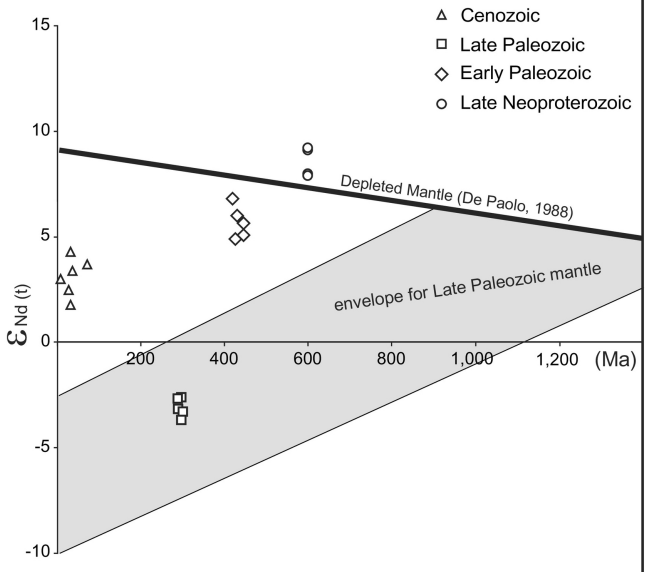


Figure 7

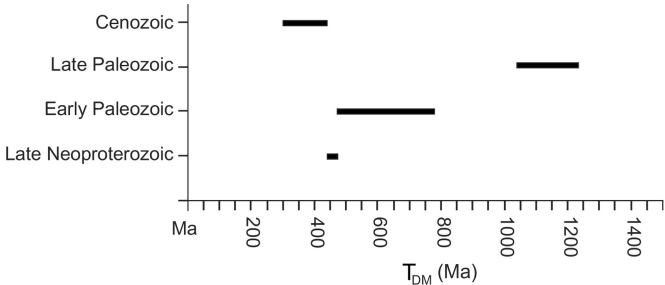


Figure 8

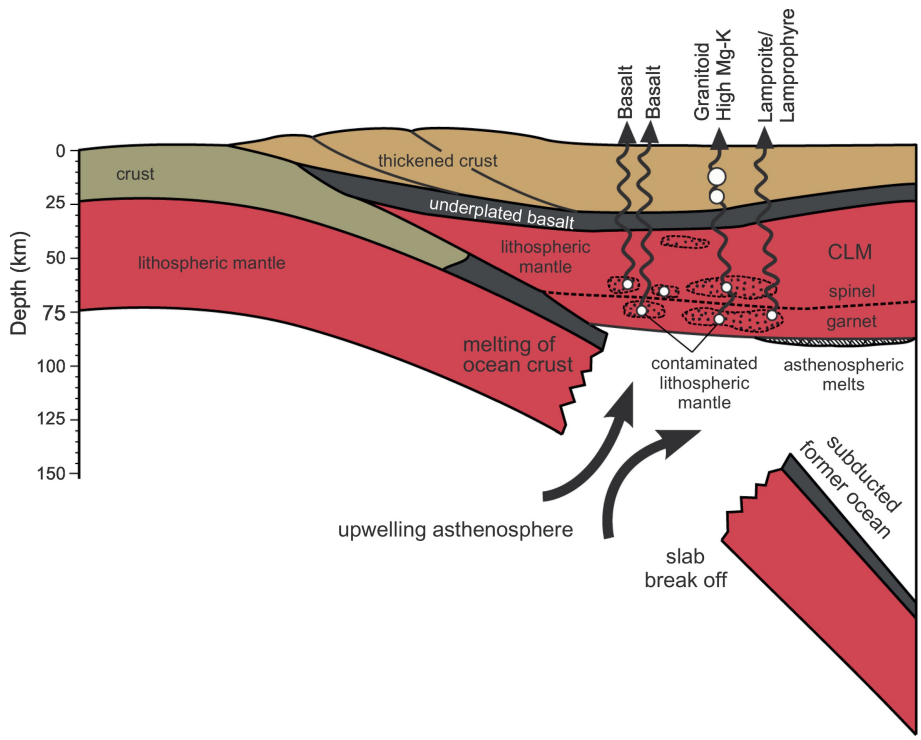


Figure 9